Study of the photodegradation of 2-bromophenol under UV and sunlight by spectroscopic, chromatographic and chemometric techniques ☆

Anusha Jayaraman[a], Sílvia Mas[a,b,∗], Romà Tauler[b], Anna de Juan[a]

[a] Chemometrics Group, Department of Analytical Chemistry, Universitat de Barcelona, Av. Diagonal, 647, 08028 Barcelona, Catalonia, Spain
[b] Environmental Chemometrics Group, Department of Environmental Chemistry, Institute of Environmental Assessment and Water Diagnostic (IDAEA-CSIC), Jordi Girona 18, 08034 Barcelona, Catalonia, Spain

ABSTRACT

This work is focused on the study of the photodegradation of 2-bromophenol under the action of UV light and sunlight. The photodegradation process has been monitored using UV–Vis spectroscopy and High Performance Liquid Chromatography coupled to diode array and mass spectrometry detectors in tandem (HPLC–DAD–MS). Multivariate resolution methods, such as Multivariate Curve Resolution-Alternating Least Squares (MCR-ALS) and hybrid soft- and hard-modeling-Multivariate Curve Resolution (HS-MCR), have been applied to the experimental data to obtain the information about the kinetic evolution and identification of the compounds involved in the photodegradation process. From the analysis of HPLC–DAD results, the complexity of the photodegradation process has been confirmed. Ten components were found to be involved in parallel, second- or higher-order reactions, which could not be ascertained from the spectroscopic results. The HPLC–MS results allowed postulating the identity of some of the compounds (such as hydroxyderivatives and bromophenol homologs) which resulted from the reactions of photohydrolysis, debromination and bromine transfer to different position of the phenol ring. The effect of the UV light and sunlight on the photodegradation process was found to affect mainly the rate of the reaction, but not the identity of the photoproducts formed. The advantages and limitations of the spectroscopic and chromatographic analysis were also discussed. The potential of combining spectroscopic and chromatographic data in a single multiset structure was also shown. This strategy, uses the advantage of the good definition of the process time axis from the spectroscopic experiment and the capability to distinguish among compounds, linked to the use of chromatographic information.

© 2012 Elsevier B.V. All rights reserved.

1. Introduction

Brominated flame retardants (BFR's) have been used since long and are persistently found in the environment, where they cause contamination and biohazard effect [1]. 2-Bromophenol is a small compound that can be formed by the thermal degradation of some flame retardants [2]. 2-Bromophenol undertakes hazardous reactions with acyl chlorides, acid anhydrides and oxidizing agents. It is used as a precursor to resorcinol and could be released to environment through waste streams. Furthermore, it has been found to cause skin, eye, mucous membranes and upper respiratory tract irritations, with varying effects depending on the duration and intensity of chemical exposure [3]. Due to these implications and the limited information about their fate in the environment, it is needed to study the chemical photodegradation of this compound.

As an environmental pollutant, 2-bromophenol is exposed to different natural radiation sources and, therefore, it is relevant to know the pathway and products derived from the photoinduced processes. Upon exposure to UV light or sunlight, the bromophenols in aquatic environment undergo photochemical changes. Preliminarily, we could expect that the UV light induced an increase in the rate of reactions with respect to the sunlight due to the shorter wavelength and higher energy of the UV radiation. However, there is no knowledge on how these different radiation sources could affect the identity of the photoproducts formed. There have been studies on the decomposition of monochlorophenols by UV irradiation [4] and under sunlight [5,6], and a study on the flash photolysis of monobromophenols [7], but a description of the kinetic pathways of bromophenols is not clear yet. Since the lowly brominated compounds were seen to undergo degradation phenomena under the action of UV light [8], a deeper study of the photodegradation of these compounds under different illuminating sources has a clear environmental relevance.

The present work attempts to study the photodegradation of 2-bromophenol under UV light and sunlight by monitoring this process with UV–Vis spectrophotometry and chromatographic techniques with UV and MS detection. The use of chromatographic and UV–Vis spectroscopic techniques helps to identify the photodegradation products and to describe their kinetic evolution. Since the process of photodegradation of these compounds is expected to be complex, chemometric tools involving multivariate analysis are used to treat the data obtained from the spectroscopic and chromatographic monitoring experiments. Multivariate Curve Resolution-Alternating Least Squares (MCR-ALS) has been used to analyze the chromatographic data [9–11]. This tool helps in determining the number of compounds present in the system and their identity through the mathematical resolution of the overlapping chromatographic peaks. Upon applying this technique, the general trend of change in concentration (peak areas) of the individual components as a function of process time can be found. This information comes from the simultaneous analysis of sampling aliquots of the 2-bromophenol solution collected at different process times. In principle, a better kinetic description of the photodegradation can be obtained by monitoring the photodegradation process spectroscopically, since many spectra can be collected in very short periods of time, spanning the process time axis in much more detail than few chromatographic aliquots. Hybrid soft- and hard-modeling-Multivariate Curve Resolution (HS-MCR) [12], a variant of MCR-ALS that allows for introducing kinetic hard-modeling information, was used to treat the spectroscopic data and provided process profiles and rate constants related to the process. However, there is a limitation linked to the sole use of spectroscopic data and it is that compounds with identical or linearly related kinetic profiles will not be distinguished. To overcome this problem, the combined analysis of spectroscopic and chromatographic data, put into a single multiset structure, has been the option adopted. Applying MCR-ALS to this combined spectroscopic/chromatographic data set allowed for modeling all components in the photodegradation process and for a better description of the kinetic evolution.

Previous studies by the research group have shown the capability of the application of HS MCR to the analysis of spectroscopic data [13,14] and of MCR-ALS to the HPLC–DAD–MS data [8], both for the photodegradation of compounds under UV light. The aim of the study of the 2-bromophenol photodegradation is providing additional insight into the evolution of pathways and mechanisms involved in this process under different kinds of light sources and the identification of the photoproducts formed. These results will help in a better understanding of the fate of this compound in the natural environment.

2. Experimental

2.1. Chemicals and solutions

2-Bromophenol (Sigma–Aldrich, Germany), acetic acid (Panreac Quimica SA, Spain), ammonium acetate (Merck, Germany) and ammonia solution (Merck, Germany), of analytical grade were used without further purification. MilliQ water of conductivity <0.05 μS/cm (Millipore) was used for the preparation of sample and reagent solutions. Methanol for HPLC from Lichrosolv® (Merck, Germany) and water for HPLC from Chromasolv® (Sigma–Aldrich, Switzerland) were used for the HPLC analysis.

The mobile phase for chromatography consisted of 50% methanol and 50% aqueous acetic acid/acetate buffer, pH 3.5. 2-Bromophenol solutions of concentrations between 1.4×10^{-4} M and 7×10^{-4} M were prepared in mobile phase by dilution of the initial liquid compound.

2.2. Apparatus

The UV light-induced bromophenol photodegradation was carried out with a setup formed by a photoreactor (Hereaus Noblelight, Germany), with a glass container (volume 0.7 L) and a 15 W UV low-pressure mercury vapor lamp, emitting predominantly at 254 nm, placed inside a quartz tube.

Sunlight bromophenol degradation was carried out using a sunlight simulating instrument (Suntest, manual CPS, Atlas) consisting of 560 cm² exposure area irradiated by an air cooled xenon arc lamp operating between 35 °C and 100 °C (Black Standard Temperature, BST). Suntest allows regulation of the irradiance and light time exposure.

Spectroscopic process monitoring was performed using a Diode array UV–Visible spectrophotometer (Agilent 8453, software: UV–Visible Chemstation). A peristaltic pump (Watson Marlon 505DU) was used for the continuous flow system between the photoreactor and the spectrophotometer in the UV-induced photodegradation experiments.

HPLC setup consisted of a High Performance Liquid Chromatography unit (Waters 2690 series, Milford, MA), a UV–Visible diode array detector (DAD, Waters 9960 series) and a benchtop triple quadrupole mass spectrometry detector (MS, Quattro LC, Micromass, Manchester, UK) connected in tandem. In the mass spectrometry detector, the ionization source was the Atmospheric Pressure Chemical Ionization (APCI) in negative mode and the software used for analysis was MassLynx V4.0. A pH-meter (pH 510, XS instruments) was used to adjust the pH of the mobile phase.

2.3. Experimental setup and procedure

2.3.1. Photodegradation studies under UV light

The bromophenol solution is irradiated under UV light in the photoreactor, while the liquid is circulated from the reactor to the spectrophotometer and vice versa. This setup forms a closed and continuous system.

2.3.1.1. Spectroscopic monitoring experiments. UV–Vis spectra of the bromophenol solution circulating from the photoreactor were collected every 30 s with a spectral resolution of 1 nm in the wavelength range of 209–450 nm.

2.3.1.2. Chromatographic monitoring experiments. Aliquots were collected from the UV photoreactor at different time intervals and analyzed with the chromatographic system. A higher number of aliquots was collected in the beginning of the process because of the faster evolution observed in the spectroscopic monitoring experiments and was gradually reduced towards the end.

The experimental conditions for chromatographic analysis included the use of a reversed phase C18 Phenomenex column, Gemini 5u 110 Å, 150 mm × 4.6 mm I.D., particle size 5 μm. 30 μL sample volume were injected and the flow of mobile phase was set at 1 mL/min with isocratic elution throughout the analysis. The eluted components were detected by a UV–Vis diode array and a mass spectrometry detector connected in tandem. The UV–DAD detector operated in a wavelength range from 190 to 400 nm with 1 nm spectral resolution and a sampling rate of 1 spectrum/s. In the MS detector, the conditions for APCI source were −3.0 kV capillary voltage, −30 V cone voltage, 150 and 500 °C source and desolvation temperatures, respectively, 48 L/h of nitrogen (99.999% purity) flow for the cone gas and 325 L/h for the desolvation gas. MS detection was performed in scan mode with an m/z range from 70 to 190, scan duration of 1 s/scan and an interscan duration of 0.1 s.
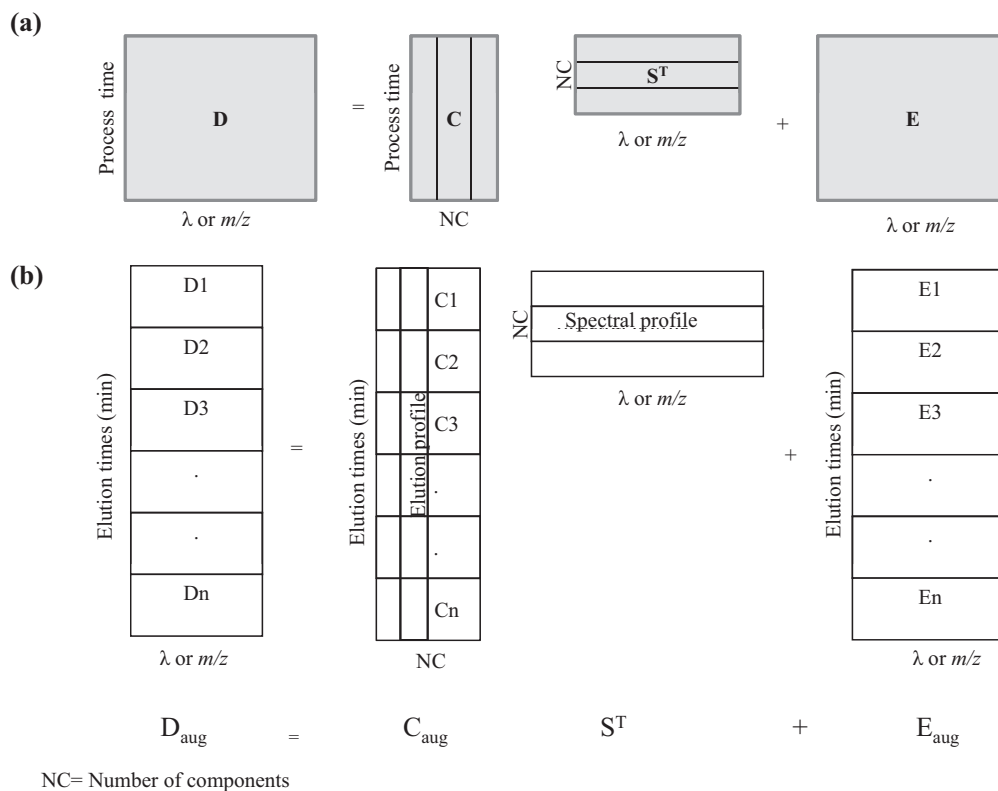
(a)

(b)

NC= Number of components

Fig. 1. (a) Bilinear model of a spectroscopic monitoring experiment-single data set structure. (b) Bilinear model of data set formed by all the chromatographic runs acquired during a process (multiset structure).

2.3.2. Photodegradation studies under simulated sunlight

The bromophenol solution was put in 20 mL quartz tubes and exposed to the xenon lamp light (irradiance set to 600 W/m^2/nm) to induce the photodegradation process. Aliquots were taken at different process times to be analyzed using the same chromatographic setup and conditions as in UV photodegradation experiments. Spectroscopic monitoring was not carried out because of the impossibility to have a continuous setup connected to the spectrophotometer and the limited volume of working bromophenol solution that could be exposed in the sunlight simulator chamber.

3. Data treatment

3.1. Data set and data structure

The measurements acquired during the spectroscopic and chromatographic monitoring experiments can be organized as data tables or raw data matrices, **D**. In the case of spectroscopic monitoring, the rows correspond to the UV–Vis spectra recorded at different process times, while the columns correspond to the kinetic traces at each wavelength (see Fig. 1a). In the case of a chromatographic run, the columns correspond to chromatograms and the rows to the detector response at the different elution times. For DAD detection, the rows are the UV–Vis spectra, whereas in the case of MS detection, the rows are the MS spectra at the different elution times.

In all the experiments mentioned, the **D** matrix obeys the bilinear model shown in Fig. 1a:

$$\mathbf{D} = \mathbf{C}\mathbf{S}^{\mathbf{T}} + \mathbf{E} \tag{1}$$

C and **S^T** contain as many profiles as pure components in the raw data set **D** (NC). In this work, the **S^T** matrix contains always the pure spectra (UV or MS) of the components involved in the photodegradation process, whereas the **C** matrix consists of the kinetic profiles

of the reaction in the spectroscopic monitoring experiments and of the elution profiles if the data set relates to a chromatographic run. The **E** matrix contains the experimental error or variance unexplained by the bilinear model.

The given bilinear model is for a single data set, such as the one of a spectroscopic monitoring experiment or that related to a single chromatographic run. When a process is monitored chromatographically, there are n data sets for the whole experiment, one per each aliquot or sample injected at a particular process time of the photodegradation. They are treated together, as a multiset structure, to get complete information about the whole experiment. For the chromatographic experiments in this study, a column-wise augmented multiset structure was chosen, as represented in Fig. 1b. **D$_{aug}$** and **C$_{aug}$** are the column-wise augmented data matrices, constructed from n **D$_i$** submatrices of raw data and n **C$_i$** submatrices of elution profiles, each pair of them related to a chromatographic run, and **S^T** is the single matrix of pure spectra, common to all chromatographic runs.

To extract more information from the experimental data, a column-wise augmented multiset structure coupling data from the spectroscopic monitoring experiment and some selected information from the chromatographic multiset with UV–DAD detection was also constructed that allowed performing a combined analysis of spectroscopic/chromatographic data.

3.2. Data pretreatment

Before proceeding to investigate to the photodegradation process, the raw data were pretreated in order to improve the quality of the signal and to reduce the data size.

Asymmetric least squares was employed to correct the baselines of HPLC–DAD chromatograms when necessary, since it can handle appropriately baselines of irregular shapes in data sets where

Table 1
General table of experiments and conditions for spectroscopic and chromatographic monitoring of 2-bromophenol photodegradation.

Experiment	Light source	Experimental technique	Conc[a] ($M \times 10^{-4}$)	Time (min)[b]	D_{DAD}	D_{MS}	N[c]
1	UV	Spectroscopy	1.4	540	**D1**	–	–
2	UV	Spectroscopy	1.4	540	**D2**	–	–
3	UV	Spectroscopy	1.4	540	**D3**	–	–
4	UV	Chromatography	1.4	90	**DC4**	–	18
5	UV	Chromatography	1.4	420	**DC5**	**DM5**	27
6	UV	Chromatography	7	420	–	**DM6**	27
7	Sun light	Chromatography	1.4	420	**DC7**	**DM7**	27
8	Sun light	Chromatography	7	420	**DC8**	**DM8**	24

[a] Conc: concentration.
[b] Time (min): total time of degradation (min).
[c] N: number of aliquots.

the significant signal (peaks) is much narrower than the baseline contribution [15].

HPLC–MS chromatographic runs were compressed in the response direction by removal of m/z channels that were noisy and unrelated to any elution peak. Such a reduction was performed by suppressing all m/z channels whose mean intensity was below 2% of the maximum intensity channels. This yielded approximately 3-fold reduction as compared with the size of the raw data set.

3.3. Resolution of experimental data: Multivariate Curve Resolution-Alternating Least Squares

Multivariate Curve Resolution (MCR) methods are used for the analysis of multicomponent systems. They aim at resolving the mixed, real, raw data matrix (**D**) into the bilinear model **CS**^{T}, formed by the pure spectra (**S**^{T}) and concentration profiles (**C**) of the underlying components [9,16]. MCR belongs to the family of soft-modeling methods, since it does not impose any mathematical model to describe the shape of the profiles in the **C** and **S**^{T} matrices. Multivariate Curve Resolution-Alternating Least Squares (MCR-ALS) is the iterative resolution method that is adopted in this study to resolve the spectroscopic and chromatographic data [9–11].

The steps of the algorithm include the determination of the number of components in **D** by rank analysis methods, such as the Singular Value Decomposition [17]. Then, an initial **C** or **S**^{T} matrix with as many profiles as the number of components estimated for **D** is constructed to start the iterative resolution process. Here, the initial **S**^{T} was found using SIMPLISMA [18]. Once the initial estimate is generated, the iterative optimization step is started. In each iterative cycle, the **C** and **S**^{T} matrices are calculated under constraints in two least-squares steps:

$$\mathbf{C} = \mathbf{DS}(\mathbf{S}^T\mathbf{S})^{-1} \quad \text{and} \quad \mathbf{S}^T = (\mathbf{C}^T\mathbf{C})^{-1}\mathbf{C}^T\mathbf{D}. \tag{2}$$

A reconstructed **D*** matrix from the product of the calculated matrices **CS**^{T} is then compared with the original **D** matrix and the iterative optimization continues until the convergence criterion is fulfilled. The convergence criterion is achieved when the variation of results between consecutive iterations goes below a preset threshold value or when a certain number of iterations are exceeded. The quality of the final MCR model can be assessed by comparing the reconstructed matrix **D*** with the raw data matrix **D**. Indicators for this purpose are the percentage of lack of fit (%LOF):

$$\%\text{LOF} = 100 \times \sqrt{\frac{\sum e_{ij}^2}{\sum d_{ij}^2}} \tag{3}$$

where e_{ij} is equal to $d_{ij} - d_{ij}^*$ (d_{ij} is an element of the raw **D** matrix and d_{ij}^* is the same element in the reconstructed **D*** matrix) and the percentage of variance explained, R^2, given by the equation:

$$R^2 = 100 \times \left(1 - \frac{\sum e_{ij}^2}{\sum d_{ij}^2} \right) \tag{4}$$

Certain constraints have to be applied in the optimization steps so as to provide meaningful shapes for the profiles in **C** and **S**^{T} and to minimize as much as possible the rotational or intensity ambiguity phenomena [11,19]. Constraints are chemical or mathematical properties that the profiles in **C** and/or **S**^{T} must fulfill. The calculated profiles are modified so that they obey the constraint condition [11]. The constraints can be applied in a flexible way [20], in **C** and/or **S**^{T} directions, differently in each profile within **C** and **S**^{T} or differently in the submatrices while using a multiset structure. The constraints used in this study are non-negativity, unimodality in elution profiles, local rank or selectivity in some elution windows [9,10,16] and spectra normalization. Hard-modeling was also used as an additional constraint by imposing a physicochemical model into the resolution and forcing the concentration profiles to obey the shapes described by a particular kinetic model. The introduction of this constraint gives rise to the hybrid soft- and hard-modeling variant of MCR (HS-MCR) that provides **C**, **S**^{T} and the related parameters (rate constants) of the hard model [12,21]. In multiset structures, the constraint of correspondence among species played a significant role, since it allowed encoding the information related to the presence/absence of some components in the different **C**$_i$ submatrices. The use of this information enabled a better definition of the pure spectra and their related concentration profiles.

In order to consider that the resolution results of an analysis are good, the variance explained must be sufficiently high and the concentration profiles and spectra obtained must be chemically meaningful and show shapes consistent with the variation in the raw data sets.

4. Results and discussion

Table 1 shows the experimental conditions of the spectroscopic and chromatographic monitoring experiments under UV and sunlight.

4.1. Spectroscopic monitoring

Spectroscopic monitoring was performed by running the photodegradation under UV light and simultaneously collecting UV–Vis spectra every 30 s. In all experiments, SVD pointed out the presence of four components. MCR-ALS was performed using spectral estimates built with SIMPLISMA and applying the constraints of non-negativity in the spectral and concentration directions, unimodality and selectivity in the concentration direction, and
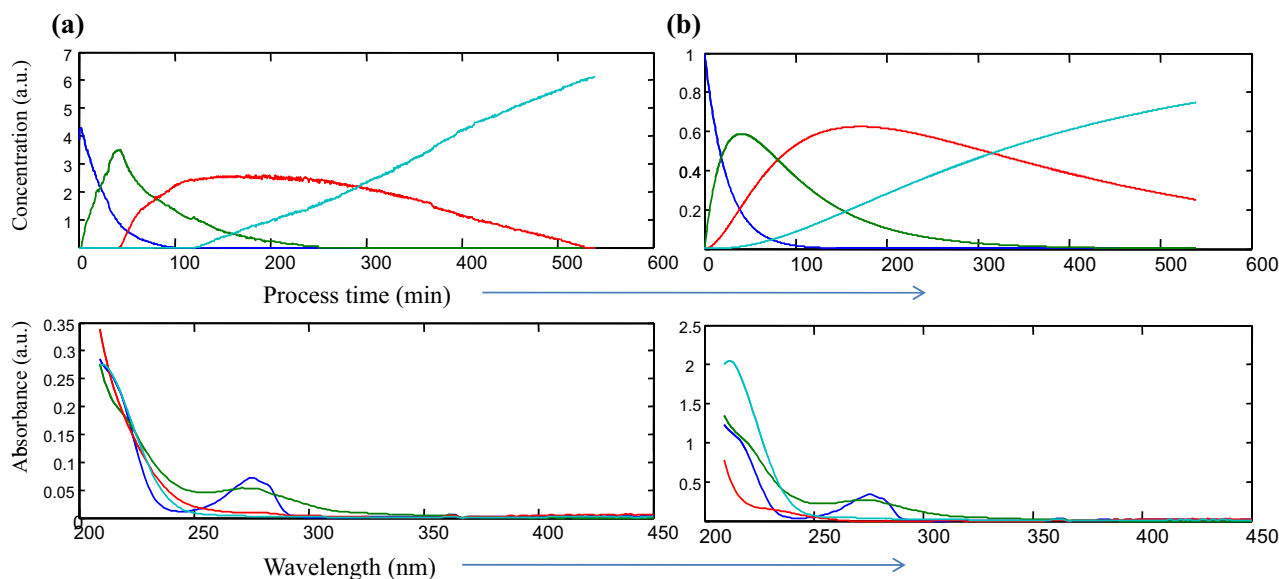
(a)

(b)

Fig. 2. Results for spectroscopic monitoring of 2-bromophenol degradation under UV light (experiment **D2**). (a) MCR-ALS kinetic profiles and related pure spectra. (b) HS-MCR kinetic profiles and related pure spectra (2-bromophenol is in dark blue. The other colors refer to photoproducts). (For interpretation of the references to color in this figure legend, the reader is referred to the web version of the article.)

normalization in the spectral direction. Fig. 2a shows the concentration profiles (**C**) and spectra (**S^T**) obtained from this analysis.

The lack of fit obtained was 1.14% and the variance explained was 99.99%. From the shape of the concentration profiles, a model of a series of first-order consecutive reactions could be postulated: $A \xrightarrow{k1} B \xrightarrow{k2} C \xrightarrow{k3} D$. HS-MCR was afterwards applied to the data and the postulated model was included as an additional hard-modeling constraint. The final information obtained by HS-MCR includes **C**, **S^T** and the rate constants. HS-MCR was also applied to the augmented data matrices of the same experiments performed on different days to obtain more accurate estimates of the parameters. Fig. 2b shows the optimized concentration and spectral profiles after HS-MCR application. Table 2 shows the quantitative results obtained by HS-MCR method. In both the MCR-ALS and HS-MCR applications, the recovered profiles, as seen from the figures of the experiment **D2**, and their values of lack of fit show good similarities. The variance explained is found to be high and, hence, satisfactory for all the experiments. This fact and the meaningful shape of concentration profiles and resolved spectra support the choice of the kinetic model applied. It is also evident that the multiset analysis has a high variance explained and shows advantages with respect to the individual analysis of experiments. Multiset analysis gives more robust results, since the flip-flop ambiguity in the single analysis of experiment **D1**, where $k2 > k1$, while in the other experiments $k1 > k2$, was solved [22]. This ambiguity may happen in experiments where the kinetic evolution follows a first-order consecutive reaction law and refers to the fact that the values of consecutive constants can be exchanged without modifying the variance explained in the dataset. This happened in experiment **D1** when analyzed alone, but it is solved in the multiset analysis.

The application of HS-MCR to the analysis of spectroscopic monitoring experiments indicates that there are only four contributions present in the system. This number of contributions would be associated straightforwardly with the number of chemical compounds in simple reaction systems. When the process is more complex, the number of detectable contributions may be lower than the real number of components due to the presence of rank-deficiency [23]. This phenomenon may occur due to the high similarity of the spectra and/or to the presence of linearly related or identical kinetic profiles among some compounds involved in the process. In order

to find out the real complexity of the photodegradation process, i.e., whether some process compounds might have been undetected, chromatographic monitoring was also carried out on this system.

4.2. Chromatographic monitoring

In the chromatographic monitoring experiments, aliquots were taken at several process times, more often in the beginning of the process because the transformation among components in the photodegradation of 2-bromophenol, both under UV and sunlight, is faster than towards the end (see Fig. 2). Table 1 describes the experimental conditions of the chromatographic experiments performed.

4.2.1. Analysis of HPLC–DAD data for UV light and sunlight photodegradation experiments

The HPLC–DAD data sets from different process times were pretreated individually to correct baselines by using asymmetric least squares, as discussed in Section 3.2. These data sets were organized in multiset structures containing chromatographic information about the different process times, so that the information from the whole process could be retained. Because of the large amount of components seen with the DAD detector in the chromatographic runs, working with the full chromatograms was avoided. Instead, different multiset structures were built for the different elution zones (windows) and MCR-ALS was applied to each of them separately [8].

Table 3 shows the quantitative resolution results for the different LC–DAD multiset structures analyzed for the photodegradation experiments carried out under UV light and sunlight.

As in spectroscopic monitoring, the number of components was determined using SVD and purest spectral estimates were selected using SIMPLISMA. The constraints applied in the MCR-ALS analysis were non-negativity in the concentration and spectral directions, unimodality for the elution profiles in the concentration direction and normalization of the resolved spectra. The total number of components resolved for the photodegradation processes is 10 in all experiments, taking into account those of all elution windows analyzed. In the analysis of the data sets at low (**D4**, **D5** and **D7**) and high (**D8**) concentration levels, the variance explained is generally satisfactory, almost always above 90%. No variation among

Table 2
Results of hybrid soft- and hard-modeling Multivariate Curve Resolution (HS-MCR) experiments.

Data matrix	NC[a]	Rate constants ($s^{-1} \times 10^{-4}$)[b]	%LOF[c]	R^{2}[d]	Constraints
D1	4	$k1 = 5.39$ (2) $k2 = 9.16$ (7) $k3 = 0.487$ (8)	2.51	99.93	Non-negativity (**C**, **S^{T}**), kinetic model
D2	4	$k1 = 6.95$ (4) $k2 = 2.202$ (7) $k3 = 0.53$ (1)	2.29	99.96	Non-negativity (**C**, **S^{T}**), kinetic model
D3	4	$k1 = 11.66$ (9) $k2 = 3.74$ (2) $k3 = 0.71$ (2)	2.98	99.91	Non-negativity (**C**, **S^{T}**), kinetic model
[D1;D2;D3] Multiset	4	$k1 = 8.21$ (8) $k2 = 3.43$ (2) $k3 = 0.60$ (2)	6.88	99.52	Non-negativity (**C**, **S^{T}**), kinetic model, correspondence among species

[a] NC: number of components.
[b] Values in parenthesis are errors associated to the kinetic fitting optimization.
[c] %LOF: percentage lack of fit.
[d] R^{2}: percentage variance explained.

the number and identity of the components was detected at the different concentration levels of the experiments performed when the same kind of light source was used.

Fig. 3a and b shows all the resolved spectral and elution profiles of the complete experiment **D5**. Fig. 3c and d shows the same results for the sunlight photodegradation experiment **D7**. The pure spectra and concentration profiles for the same compound share the same color in the figures. These plots contain the overlapped results of all window multisets analyzed.

As can be seen in both UV and sunlight photodegradation, many resolved spectra are very similar among components. These components could be resolved because of the difference among their elution behaviors and the fact that the different elution time windows were treated separately. Fig. 3b and d give a first impression of the kinetic evolution of the resolved components through the changes in intensity of the elution profiles along the process runs.

Table 3
UV light and sunlight photodegradation – results from HPLC–DAD.

Data matrix	Number of components	% Variance explained (R^{2})
UV light photodegradation experiment		
DC4 Time window (min):	10	
1.001–3.24	4	96.95
3.25–4.76	3	96.36
6.008–7.74	1	92.16
7.76–9.9	1	99.95
10.51–12.75	1	65.87[a]
DC5 Time window (min):	10	
1.001–3.24	4	97.79
3.25–4.76	3	96.33
6.008–7.74	1	95.60
7.76–9.9	1	99.90
10.51–12.75	1	90.15
Sunlight photodegradation experiment		
DC7 Time window (min):	10	
1.001–3.24	3	90.87
3.25–4.76	4	99.88
6.008–7.74	1	93.89
7.76–9.9	1	99.98
10.51–12.75	1	96.43
DC8 Time window (min):	10	
1.001–3.24	4	99.88
3.25–4.01	2	98.04
4.01–4.76	1	99.99
6.008–7.74	1	96.68
7.76–9.9	1	99.99
10.51–12.75	1	99.46

[a] Low variance explained is due to the low signal-to-noise ratio (s/n) of the minor compound modeled.

Please note that the total duration of the experiment **DC4** is much shorter than the rest of experiments.

For UV photodegradation, the decay of 2-bromophenol (dark blue profile) is fast, many intermediate species emerging and decaying are detected, and a few components keep increasing until the end of the process. In the case of sunlight photodegradation, the parental compound 2-bromophenol decays much more slowly. The evolution of intermediate components, with emergence-decay evolution, is seen until the end of the monitored process time. End products are formed in a lower proportion than under UV light for the same time scale. For clarity, Fig. 4a and b shows the kinetic evolution of the components in the photodegradation process by displaying the variation of the peak area of the different resolved components as a function of the process time. The differences between the photodegradation rate under different light sources can be seen in the evolution of the parental compound, 2-bromophenol (1), which decays faster in UV light (in about 70–90 min) than in sunlight, where it takes about 200–230 min.

Table 4 shows the retention times of the peaks in UV and sunlight experiments (the number indicates the related components in Fig. 4). Upon comparing the retention times and the related resolved spectra of the two experiments, it can be seen that photodegradation under the two sources of light yields many similar components. As seen from Table 4, components 1, 2, 3, 4, 5, 6 and 7 from UV light degradation have similar retention times and spectral profiles to the corresponding components from the sunlight experiment. Components found to be different in both photodegradations are usually very minor (8_{sun}, 9_{sun} in sunlight and 8_{UV} in UV) or may be simply not formed in a large enough extent under sunlight (9_{UV} and 10_{UV} from UV photodegradation). Also, the values of correlation coefficients obtained between the resolved spectra of the components from the two experiments (Table 4) supports the similarity between them and are found to be higher than 0.98 for almost all the similar components.

It is worth noticing that the chromatographic monitoring clearly showed high similarity in the kinetic evolution of some components and allowed for the detection and modeling of very minor photoproducts. These two factors help to understand why the number of contributions detected in the analysis of the sole spectroscopic monitoring experiments was lower. On one hand, compounds with very similar or identical kinetic evolution could not be distinguished. On the other hand, very minor compounds could not be modeled due to very little contribution to the global mixed signal of the spectra collected at different process times.

4.2.2. Analysis of HPLC–MS results for UV light and sunlight experiments

HPLC–MS data were structured in a multiset structure and pretreated by compressing the dataset in the column direction to
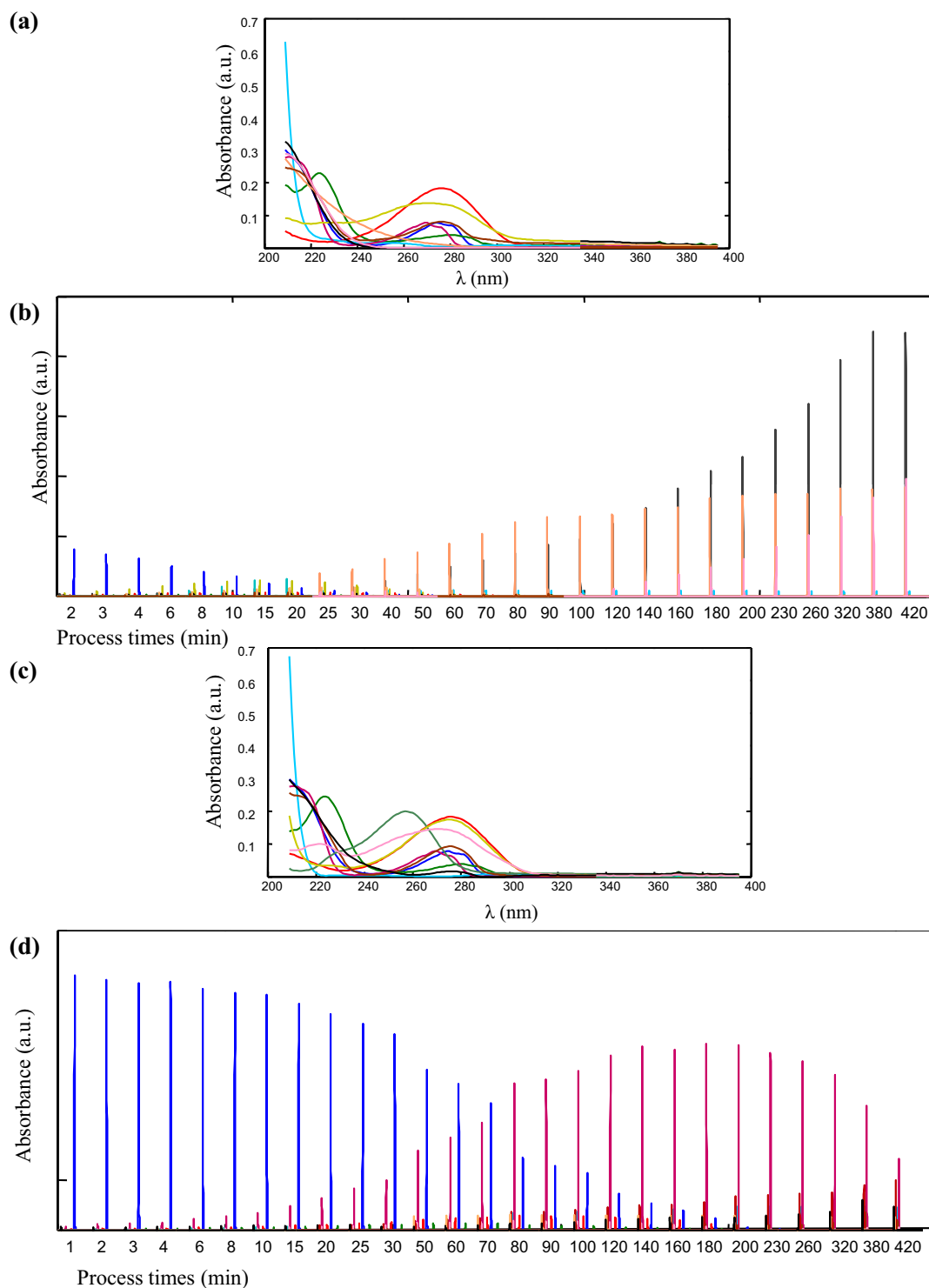
Fig. 3. MCR-ALS results of chromatographic monitoring of 2-bromophenol degradation under UV light (experiment **D5**). (a) Resolved elution profiles and (b) spectra. MCR-ALS results for experiment **D7** (sunlight photodegradation). (c) Resolved elution profiles and (d) spectra.

remove the irrelevant m/z channels. Because of the lower number of components detected with HPLC–MS in this photodegradation system, a single multiset structure was analyzed.

The procedure for resolving HPLC–MS profiles was the same as for the HPLC–DAD multisets. The only difference was that the constraint of unimodality could not be applied, since isomers could provide more than one elution peak related to the same resolved MS spectrum. Table 5 shows the results from the

analysis of HPLC–MS data from UV light and sunlight experiments.

The variance explained in the analysis of HPLC–MS data is satisfactory, taking into account the higher noise level of this kind of measurement. The same number of contributions was detected under the two different sources of light. Increasing the concentration of the sample (Expts **DM6**, **DM8**) did not help in the detection of additional components. Three different contributions, i.e., three
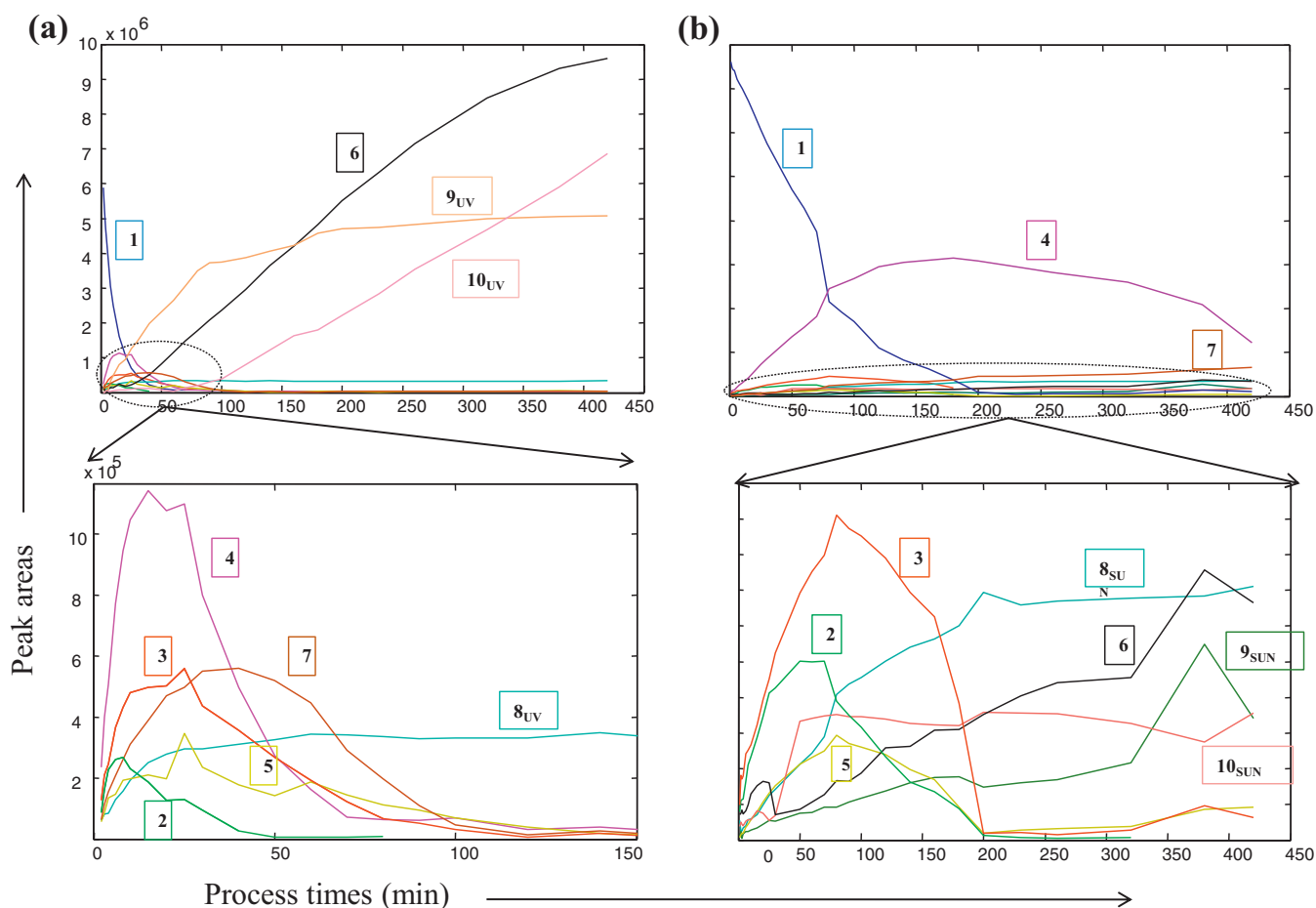
Fig. 4. Plots of peak areas of resolved components as a function of process time for the 2-bromophenol photodegradation. (a) Degradation under UV light (experiment **DC5**) and (b) degradation under sunlight (experiment **DC7**).

different MS spectral signatures, related to chemical compounds were detected in the HPLC–MS data.

The smaller number of contributions detected by HPLC–MS, as compared with HPLC–DAD, is due to the high noise level of the MS detection used that made infeasible the detection of some minor components and to the fact that homolog compounds share the same MS spectrum and are, therefore, modeled as a single contribution in the MCR-ALS results. The HPLC–MS results were used for identification purposes only, because the higher noise level prevented the resolution of minor peaks.

Since the ionization source in the MS detector used was the APCI in negative mode, the components are identified by the molecular weight of the deprotonated molecular ion $[M-H]^-$. With the knowledge of the molecular weight, some of the components could be identified or, at least, assigned to potential components. The compound with $[M-H]^-$ value 109, could be resorcinol (3-hydroxyphenol), 4-hydroxyphenol, as identified by Lipczynska [7] or 2-hydroxyphenol, explained as formed by photohydrolysis [24]. It could also be attributed to cyclopentadienic acid, as reported by Guyon, formed due to the photocontraction by irradiation through a Wolff's rearrangement and hydrolysis, a reaction observed also in 2-chlorophenol [25]. All these compounds were found in previous studies that reported the debromination as a usual phenomenon in the photodegradation of 2-bromophenol. There were two homologous components having the same MS spectrum, with $[M-H]^-$ value at 171/173 and another peak at 79/81. These compounds were the parental 2-bromophenol, where the $[M-H]^-$ 171/173 corresponds to the molecular mass of 2-bromophenol and 79/81

Table 4
Retention times of peaks resolved in the 2-bromophenol degradation under UV light and sunlight (HPLC–DAD data).

UV light photodegradation (experiment **D5**)		Sunlight photodegradation (experiment **D7**)		Correlation coefficient, R^2
Component numbers	Retention times	Component numbers	Retention times	
1	8.74–8.8	1	8.608–8.792	1.0000
2	12.07–12.2	2	11.9–12.22	0.9913
3	6.89–6.94	3	6.725–6.842	0.9939
4	4.29–4.3	4	4.242–4.292	0.9998
5	3.84–3.857	5	3.808–3.858	0.9172
6	2.023–2.073	6	2.075	0.9884
7	2.907–2.923	7	2.892–2.925	0.9947
8_{UV}	3.457–3.64	8_{sun}	3.708–3.725	–
9_{UV}	1.807–1.823	9_{sun}	3.558–3.575	–
10_{UV}	2.29–2.323	10_{sun}	2.175–2.192	–

Table 5
Results from HPLC–MS, UV light and sunlight experiments.

Data matrix	Number of components	*m/z* values	Retention times (min)	R^2
UV light photodegradation experiment				
DM5	3(4[a])	171/173, 79/81	8.2–9.6, 11.5–13.2	86.36
		79/81	1.6–2.4, 3.3–4.3	
		109	2.6–4.7	
DM6	3	171/173, 79/81	8.2–9.6, 11.5–13.2	94.67
		79/81	1.6–2.4, 3.3–4.3	
		109	2.6–4.7	
Sunlight photodegradation experiment				
DM7	3(4[a])	171/173, 79/81	8.2–9.6, 11.5–13.2	93.07
		79/81	3.3–4.3	
		109	2.6–4.7	
DM8	3(4[a])	171/173, 79/81	8.2–9.6, 11.5–13.2	97.3
		79/81	3.3–4.3	
		109	2.6–4.7	

[a] Background contribution had to be included as the fourth component in order to obtain a better resolution of the three chemical contributions in some data sets.

corresponds to the bromine isotopes, and 4-bromophenol, which can be formed by the bromine transfer phenomenon upon UV irradiation observed by Akai et al. [26]. Further evidence from previous studies performed in the research group confirmed also the presence of this compound [8]. The other two components with a smaller [M−H]⁻ value at 79/81, found in the photodegradation under UV light, are also observed to be homologs. In the case of sunlight experiment, their presence is lower than for UV photodegradation, since those were the last photoproducts formed during the degradation process. These photoproducts could be identified as HBr or as small brominated aliphatic compounds, in agreement with the reported formation of HBr upon flash photolysis of bromophenols [24]. The assignments of the different compounds found are in agreement with a previous study [8].

The retention times of the components identified by HPLC–MS and HPLC–DAD also show similarities among the components identified with the two detection systems. Also, most of the components detected in the experiments under UV light were similar to those under sunlight. The missing compound in the sunlight degradation, related to *m/z* values 79/81, may be undetected because this is one of the last photoproducts formed in the UV photodegradation and may have not yet appeared at this process time under sunlight. Thus, the main effect of the different light sources on the photodegradation of 2-bromophenol is linked to the rate of the photodegradation process, but not to the identity of the photoproducts formed.

4.3. Spectroscopic/chromatographic coupling analysis

As an attempt to extract more information from the experimental data collected during the 2-bromophenol photodegradation under UV light, MCR-ALS was performed onto a multiset structure formed by spectroscopic and chromatographic information.

When this structure is analyzed by MCR-ALS, both potential ability to detect and model all the components and to define in detail the process evolution are kept. This is due to the simultaneous use of the uncorrelated chromatographic/elution information and the well-defined process time axis provided by the spectroscopic experiment.

In order to perform the combined spectroscopic/chromatographic data analysis, a column-wise augmented multiset structure is constructed with the spectroscopic monitoring experiment and some selected information from the chromatographic multiset. From the chromatographic multiset, only a few elution time windows most representative of the elution profiles of the different components are introduced to perform the combined MCR-ALS.

Fig. 5a shows the structure of the combined multiset formed by the spectroscopic data and the selected elution time windows of the chromatographic monitoring data.

D_{aug} represents the augmented data structure. D_{aug} is formed by S_p, which contains represents the spectroscopic monitoring data and T_w's, which are the time windows selected from the chromatographic multiset. T_{w1}, T_{w2} and T_{w3} correspond to elution time windows 1, 2 and 3, where a single compound was eluting. For these so well defined components, only the time window related to the chromatographic run where these components are more dominant is included in the multiset structure. For time windows in which several components were coeluting, time windows from two chromatographic runs are included to have more information about these components in the resolution. These are the two sections labeled T_{w4} and T_{w5} in Fig. 5a. Before starting the MCR-ALS analysis, the different submatrices in the augmented matrix D_{aug} are scaled to minimize signal intensity differences in the multiset structure.

The initial estimates for this combined analysis were the resolved spectra from the chromatographic multiset. The constraints applied were non-negativity along spectral and concentration directions, unimodality along concentration direction, normalization along spectral direction and correspondence among the species. The correspondence among species plays an important role in this kind of analysis, since selectivity (in T_{w1}, T_{w2} and T_{w3}) and absence of many components (in T_{w4} and T_{w5}) can be set for the different elution time submatrices. For the spectroscopic experiment (S_p), all the species are considered to be present. The selectivity and local rank information from the chromatographic time windows provides a better quality to the final resolution results of the multiset structure and a drastic decrease of the rotational ambiguity, a common uncertainty phenomenon in MCR methods [11,27].

In this study, the combined analysis was performed for the spectroscopic data and the elution time windows of the chromatographic monitoring data from experiment **DC5**. Spectra collected every 30 s during the first 90 min of the experiment **DC5** were used for the spectroscopic part of the combined analysis (S_p) since the parental 2-bromophenol and most other components in the process have emerged and decayed during this time range (see plot of peak area vs. process time in Fig. 4a). Taking only this period of time, the minor components evolving at the beginning of the process are also better represented.

Fig. 5b shows the resolved concentration and spectral profiles for the combined analysis. The variance explained was 99.02%, which was satisfactory and confirmed the good description of the multiset structure by the MCR-ALS model. In this case, 8 out of
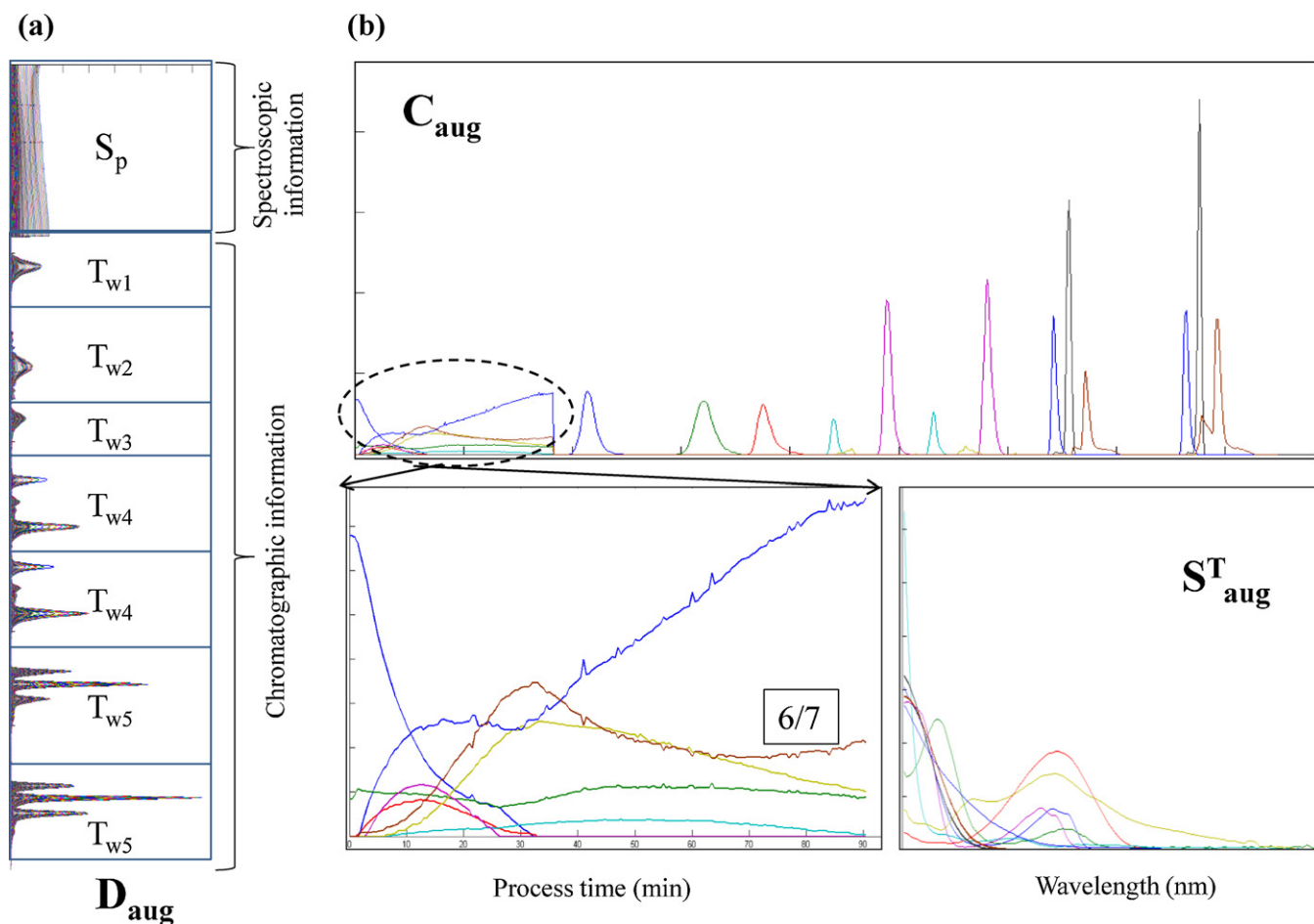
Fig. 5. Analysis of spectroscopic/chromatographic multiset linked to 2-bromophenol photodegradation under UV light. (a) Multiset structure (see text for meaning of D_{aug} submatrices). (b) Resolved concentration and spectral profiles of coupling analysis (kinetic profiles of spectroscopic monitoring have been zoomed in for a better view).

the 10 components resolved chromatographically provided acceptable concentration profiles in the spectroscopic experiment, with shapes in agreement with those observed in the peak area vs. process time plot (in Fig. 4a). Only a very minor compound co-eluting in T_{w4} was not detected and the components colored in brown and black in Fig. 5b appeared as a single profile (brown) in the spectroscopic experiment. This last problem is due to the high similarity in the kinetic and spectral profiles for these components and to the fact that both co-elute in the chromatographic window. Nevertheless, the description of the kinetic evolution in the spectroscopic experiment is much better than the results obtained when this experiment was analyzed alone.

From the kinetic profiles obtained, it can be concluded that 2-bromophenol photodegradation takes place through a complex process, where the kinetic evolution of many components is very similar. This can suggest the presence of many parallel or second- or higher order reactions. At this point, no more detail on the mechanism can be provided since not all the components could be identified and, therefore, there is a lack of knowledge about the underlying chemistry behind this photodegradation process. For processes with a slightly smaller number of components involved and a deeper knowledge of the underlying chemistry, the multiset structure presented would have allowed the postulation of a kinetic model for the spectroscopic experiment (introduced as an additional constraint) [28].

For the process presented, there would be a massive number of possible models that could fit the data and there are no sufficient sound chemical reasons to choose one of them over the rest.

Therefore, the soft-modeling chromatographic/spectroscopic data analysis is the alternative that can provide the most reliable results.

5. Conclusions

The differences of using UV or sunlight for the 2-bromophenol photodegradation were shown to be mainly on the rate of the photodegradation, whereas both light sources yielded similar photoproducts among which hydroxyphenol, 4-bromophenol, were identified.

As general conclusions on the monitoring of photodegradation processes, it has been shown that spectroscopic experiments allow for a good description of the mechanism and evolution of processes because of the detailed monitoring in time. However, the number of process contributions can be underestimated when components with identical or very similar spectra and/or kinetic evolution exist. Chromatographic monitoring coupled with MCR-ALS is a good strategy to distinguish components with similar kinetic evolution and similar spectra because of their differences in elution pattern. It can also detect minor components because their signals are not mixed with the rest of the components. The only drawback in the chromatographic monitoring is the poorly defined process time axis because of the limited number of chromatograms linked to the process. The combined analysis of spectroscopic and chromatographic monitoring data sets by MCR-ALS provides a more detailed description of the kinetic evolution of the process due to the good description of the process time axis in the spectroscopic data set and to the distinct information among components incorporated

from the chromatographic data. Only in very complex processes with a large number of compounds, a few contributions may be missed if some compounds are very minor or if they are similar in kinetic, spectral and elution behaviors. For processes with a low number of compounds or with a well known chemistry, it is possible to incorporate kinetic models to fit the concentration profiles in the spectroscopic monitoring experiment. In these cases, a full description of the process mechanism and products formed is possible.

Acknowledgments

References

[1] C.A. de Wit, Chemosphere 46 (2002) 583.
[2] M. Uchida, M. Furusawa, A. Okuwaki, J. Hazard. Mater. 101 (2003) 231.
[3] http://toxnet.nlm.nih.gov/, Hazardous Substances Databank (Number: 7648), Toxicology Data Network (last updated: 26-06-2009).
[4] Y. Ku, R.M. Leu, K.C. Lee, Water Res. 30 (1996) 2569.
[5] J. Klánová, P. Klán, J. Nosek, I. Holoubek, Environ. Sci. Technol. 37 (2003) 1568.
[6] K.H. Wang, Y.H. Hsieh, K.S. Huang, J. Chin. Inst. Environ. Eng. 4 (1994) 111.
[7] E. Lipczynska-Kochany, Chemosphere 24 (1992) 911.
[8] S. Mas, A. Carbó, S. Lacorte, A.d. Juan, R. Tauler, Talanta 83 (2010) 1134.
[9] A. de Juan, R. Tauler, Crit. Rev. Anal. Chem. 36 (2006) 163.
[10] R. Tauler, Chemom. Intell. Lab. Syst. 30 (1995) 133.
[11] R. Tauler, A. Smilde, B. Kowalski, J. Chemom. 9 (1995) 31.
[12] A. de Juan, M. Maeder, M. Martinez, R. Tauler, Chemom. Intell. Lab. Syst. 54 (2000) 123.
[13] M. De Luca, S. Mas, G. Ioele, F. Oliverio, G. Ragno, R. Tauler, Int. J. Pharm. 386 (2010) 99.
[14] S. Mas, A. de Juan, S. Lacorte, R. Tauler, Anal. Chim. Acta 618 (2008) 18.
[15] P.H.C. Eilers, H.F.M. Boelens, in: Biosystems Data Analysis Group, Amsterdam, 2005, http://www.science.uva.nl/~hboelens/publications/draftpub/Eilers_2005.pdf.
[16] S.C. Rutan, A. de Juan, R. Tauler, in: S.D. Brown, R. Tauler, B.W. (Eds.), Comprehensive Chemometrics, vol. 2, Elsevier, Amsterdam, 2009, p. 249.
[17] G.H. Golub, C.F.v.V. Loan, Matrix Computations, The John Hopkins University Press, London, 1989.
[18] W. Windig, Chemom. Intell. Lab. Syst. 16 (1992) 1.
[19] H. Abdollahi, R. Tauler, Chemom. Intell. Lab. Syst. 108 (2011) 100.
[20] A. de Juan, Y. Vander Heyden, R. Tauler, D.L. Massart, Anal. Chim. Acta 346 (1997) 307.
[21] R. Tauler, M. Maeder, A. de Juan, in: S.D. Brown, R. Tauler, B. Walczak (Eds.), Elsevier, Amsterdam, vol. 2, 2009, p. 473.
[22] J. Andraos, Can. J. Chem. 77 (1999) 565.
[23] J. Saurina, S. Hernández-Cassou, R. Tauler, A. Izquierdo-Ridorsa, J. Chemom. 12 (1998) 183.
[24] H.I. Joschek, S.I. Miller, J. Am. Chem. Soc. 88 (1966) 3269.
[25] C. Guyon, P. Boule, J. Lemaire, Tetrahedron Lett. 23 (1982) 1581.
[26] N. Akai, S. Kudoh, M. Takayanagi, M. Nakata, Chem. Phys. Lett. 363 (2002) 591.
[27] R. Tauler, M. Maeder, in: S.D. Brown, R. Tauler, B. Walczak (Eds.), Elsevier, Amsterdam, vol. 2, 2009, p. 345.
[28] S. Mas, R. Tauler, A. de Juan, J. Chromatogr. A 1218 (2011) 9260.